AIP Applied Physics Letters

GaN-based high contrast grating surface-emitting lasers

Tzeng-Tsong Wu, Shu-Hsien Wu, Tien-Chang Lu, and Shing-Chung Wang

Citation: Applied Physics Letters **102**, 081111 (2013); doi: 10.1063/1.4794081
View online: http://dx.doi.org/10.1063/1.4794081
View Table of Contents: http://scitation.aip.org/content/aip/journal/apl/102/8?ver=pdfcov
Published by the AIP Publishing

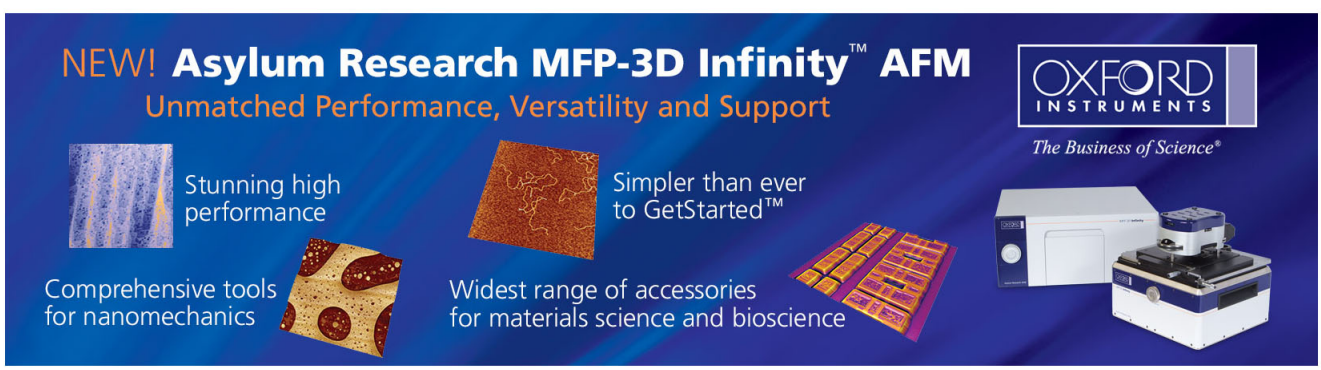

GaN-based high contrast grating surface-emitting lasers

Tzeng-Tsong Wu, Shu-Hsien Wu, Tien-Chang Lu,[a] and Shing-Chung Wang
Department of Photonics & Institute of Electro-Optical Engineering, National Chiao Tung University, Hsinchu 30050, Taiwan

(Received 10 September 2012; accepted 18 February 2013; published online 27 February 2013)

GaN-based high contrast grating surface-emitting lasers (HCG SELs) with AlN/GaN distributed Bragg reflectors were reported. The device exhibited a low threshold pumping energy density of about 0.56 mJ/cm^2 and the lasing wavelength was at 393.6 nm with a high degree of polarization of 73% at room temperature. The specific lasing mode and polarization characterisitcs agreed well with the theoretical modeling. The low threshold characteristics of our GaN-based HCG SELs faciliated by the Fano resonance can serve as the best candidate in blue surface emitting laser sources. © *2013 American Institute of Physics*. [http://dx.doi.org/10.1063/1.4794081]

Sub-wavelength high contrast gratings (HCGs) with the periodic index difference structure have been widely investigated in recent years owing to their advantageous properties. By modifying HCG parameters such as the grating height, period and width, high reflectivity reflectors with broad stop-band width, and specific polarization could be achieved and applied for many applications.[1–5] For example, the HCGs have been integrated with vertical cavity surface-emitting lasers (VCSELs) such as 850 nm GaAs and 1550 nm InP VCSELs as the top mirrors. The HCGs serve not only as high reflectivity reflectors but also allow controlling of polarization, tuning of wavelength with a fast modulation speed.[2,5] On the other hand, the HCGs have been used as in-plane, large area, high-quality factor (Q) resonators.[6,7] GaAs-based membrane HCG high-Q resonators were reported with a Q value of 14 000 under optical pumping.[7] However, wide bandgap materials such as GaN-based HCG surface-emitting lasers (HCG SELs) have not been reported so far.

GaN-based VCSELs and photonic crystal surface emitting lasers (PCSELs) have been reported earlier.[8–14] However, fabrication of high Q resonators for these lasers requires rather difficult process with poor reproducibility. In comparison, the high Q membrane HCGs could be realized through relatively simple fabrication process. Besides, the HCG resonators can provide additional advantages to control the emission polarization and emission wavelength. However, it is still a technical challenge to fabricate GaN-based membrane HCG structures due to the immature etching process to make suspended GaN membrane.[15] In this work, we report the design, fabrication, and lasing characteristics of GaN-based HCG SELs at room temperature under optical pumping. The GaN-based HCG SELs showed a low threshold energy density of 0.56 mJ/cm^2 with a high degree of polarization (DOP) of 73%. Besides, the specific lasing modes agreed with the band diagram and mode pattern calculated by plane wave expansion (PWE)[16] and finite element methods (FEM).[17]

Schematics of GaN-based HCG SELs are shown in Fig. 1(a). The device consists of two main parts. First part is the epitaxial structures, consisting of a 25-pair AlN/GaN distributed feedback reflector (DBR), a 320 nm-thick n-GaN layer, 10 pairs of InGaN/GaN multiple quantum wells (MQWs), and a 100 nm-thick p-GaN layer. The detailed growth parameters were reported elsewhere.[12] The bottom AlN/GaN DBR can play an important role as the low refractive index layer for confining the optical mode in the HCG cavity without using the suspended membrane structure. The typical photoluminescence (PL) spectrum of MQWs had a peak centered at 405 nm with a linewidth of about 25 nm.

The second part is the HCG structure. The parameters of HCG structure were designed and calculated by rigorous coupled-wave analysis (RCWA).[18] The asymmetric reflectivity spectra as functions of different duty cycle (the grating width divided by the grating period) and grating height for the TE polarization of the GaN-based HCG were analyzed. First, the grating period was designed to be 345 nm to bring the Fano resonance approaching to the GaN gain peak. Fig. 1(b) shows the calculated reflectivity spectra mapping as a function of duty cycle. Clearly, the duty cycle of HCG resulted in the peak shift of reflectivity spectra. To match the target wavelength of about 400 nm, the duty cycle was set to be around 0.8 to 0.86, which is allowed for the fabrication tolerance. Fig. 1(c) shows the calculated reflectivity spectra mapping versus the grating height. The calculated results show that the number of reflectivity peaks would increase with increasing the grating height due to the onset of higher order Fabry-Perot modes. In order to fit our target wavelength, the grating height was selected to be around 490 to 530 nm which was close to a 3λ cavity length. Fig. 1(d) shows the reflectivity spectrum when the grating period, height, and duty cycle were set to be 345 nm, 520 nm (3λ cavity), and 0.82. The reflectivity spectrum shows an asymmetric line shape from 0 to 1 which was referred to the feature of Fano resonance.[19,20] Fano resonance caused by two wave interference from different channels would form the asymmetric line shape spectrum. For GaN-based HCG SELs, the first optical channel is the Bragg scattering induced by HCG in the lateral direction. The Bragg scattering would cause a narrow band width spectrum. The second optical channel is the Fabry-Perot scattering induced by the index difference in the vertical direction. The Fabry-Perot scattering would generate a flat band spectrum. These two different channels would reach the same final state resulting in an asymmetric line shape of the spectrum.[6,7] Moreover, this

[a]Electronic mail: timtclu@mail.nctu.edu.tw.

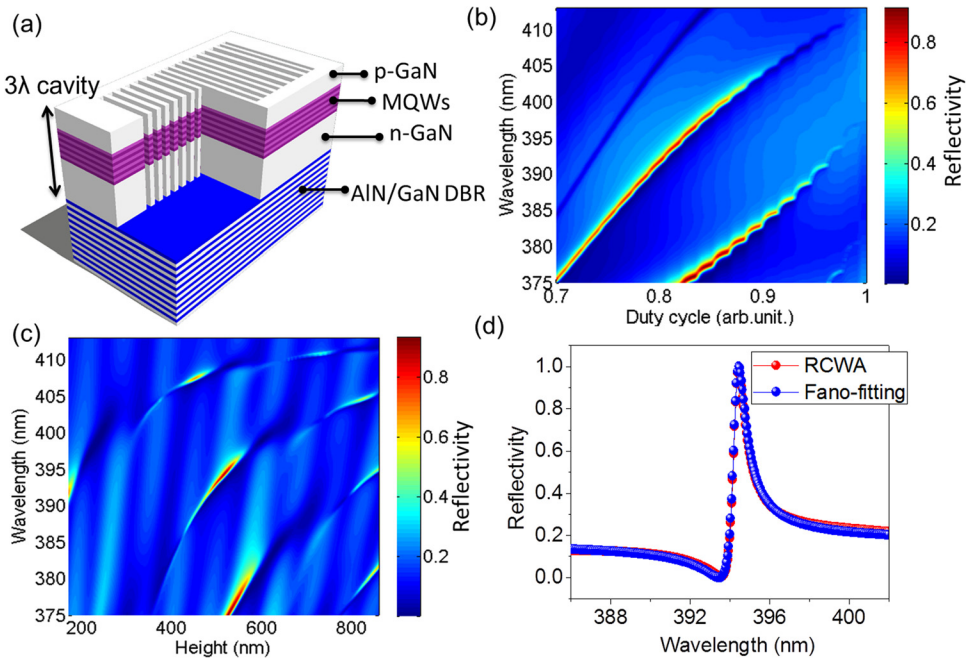

FIG. 1. (a) Schematics of GaN-based HCG SELs. (b) Reflectivity spectra mapping as a function of duty cycle (the grating width divided by the grating period). (c) Reflectivity spectra mapping versus grating height. (d) The reflectivity spectra for the grating with period: 345 nm, filling factor: 0.82, grating height: 520 nm. The red and blue lines show the simulation results by RCWA and fitting results by the Fano resonance equation.

phenomenon could confine the optical mode in the structure well and result in a high Q factor, which is beneficial for the laser operation. The simulated reflectivity spectrum can be compared to the Fano resonance equation,[6,7]

$$F(\Omega) = \frac{1}{1+q^2}\frac{(\Omega+q)^2}{\Omega^2+1}, \quad \Omega = \frac{2(\omega-\omega_0)}{\gamma}, \qquad (1)$$

where ω_0 and γ are the center frequency and the width of the narrowband, q is the Fano asymmetry parameter. The Q factor of the cavity can be calculated using $Q = \frac{\omega_0}{\gamma}$. The blue curve in Fig. 1(b) representing the fitted Fano resonance curve based on Eq. (1) matches quite well with the simulated reflectivity spectra obtained by RCWA. The extracted Q factor, in this case, was calculated to be 533.

For fabrication of the HCG SEL device, the as-grown sample first deposited a 300 nm-thick SiN_x layer as a hard mask by the plasma-enhanced chemical vapor deposition (PECVD) and was spin-coated the poly-methyl methacrylate (PMMA) photoresist. The HCG structure was patterned by electron-beam lithography on the PMMA, and then etched by reactive ion etching (RIE) down to the SiN_x layer. The HCG patterns were etched down to penetrate the MQWs layer of about 490 nm using inductively coupled plasma (ICP) dry etching. The total area of HCG region was about 20 μm^2. Fig. 2 shows the planer and tilted angle scanning electron microscope (SEM) images of the device. It can be seen that the period, duty cycle, and height of HCG were estimated to be 345 nm, 0.82, and 490 nm, respectively. The fabricated GaN-based HCG SEL device was tested under room temperature conditions. A 355 nm pulse Nd:YVO_4 laser with a pulse width of ~0.5 ns at a repetition rate of 1 kHz was used as the optical pumping source. The laser beam with a spot size of about 20 μm to cover the HCG pattern was obliquely incident onto the device. The μ-PL signal was collected by a 15× objective lens normal to the sample surface or by a fiber with a 600 μm core in the normal plane of the sample. The collected signal was then fed into a spectrometer (Jobin-Yvon IHR320 Spectrometer) with a spectral resolution of about 0.07 nm.

The pumping energy density versus the light output characteristics curve is shown in Fig. 3(a). A clear threshold can be observed when the threshold energy density was about 0.56 mJ/cm^2. This threshold pumping energy density is substantially lower compared to that of previously reported values, 3.5 mJ/cm^2 of GaN-based PCSELs[12] and 1.15 mJ/cm^2 of GaN-based VCSELs.[9] The low threshold condition could be attributed to the perfect mode confinement in HCG structures under Fano resonance.[21] The inset of Fig. 3(a) shows the CCD image of the lasing area of the

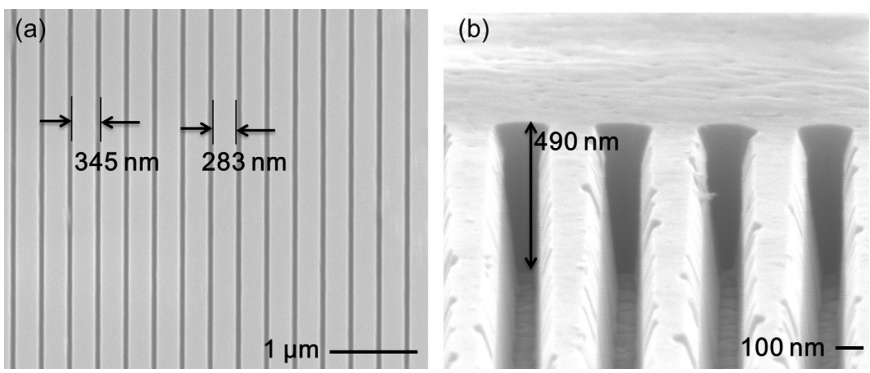

FIG. 2. (a) Top-view and (b) tilted angle SEM images of GaN-based HCG SELs. The period, duty cycle, and height of HCG were estimated to be 345 nm, 0.82, and 490 nm, respectively.

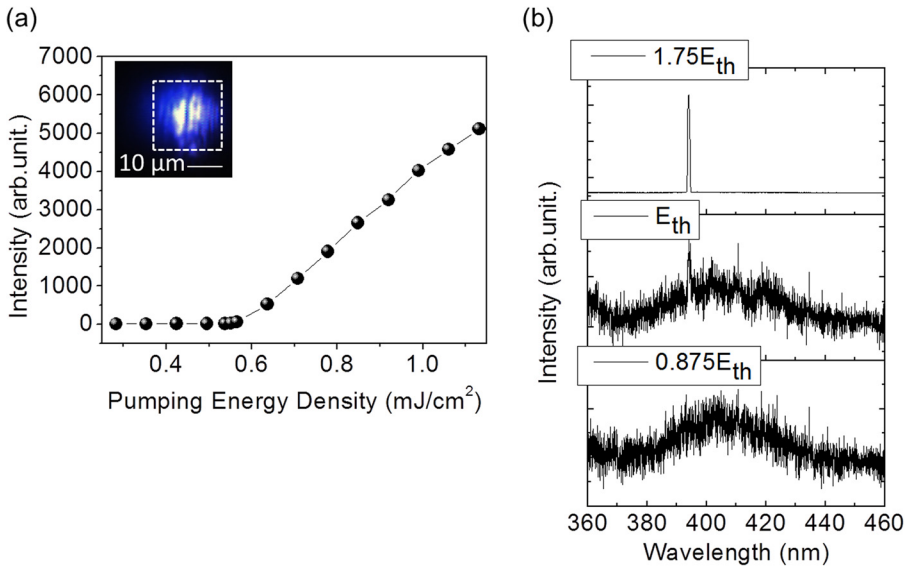

FIG. 3. (a) The input-output characteristics of GaN-based HCG SELs. The inset shows the CCD image when the GaN-based HCG SEL was above the threshold condition. (b) The measured spectra with different pumping powers of 0.875 E_{th}, E_{th} and 1.75 E_{th}. The FWHM of lasing peak at 1.75 E_{th} is 0.88 nm.

device pumped above the threshold. The lasing area was almost covered the whole HCG area marked as the white dashed line. Fig. 3(b) shows the lasing spectra with different pumping energy densities. When it was above the threshold condition, one dominated lasing peak at 393.6 nm was observed with a full width at half maximum (FWHM) of about 0.88 nm. The emission spectrum right below the threshold condition is plotted in Fig. 4. The spectrum with black curve exhibits an asymmetric line shape, which is the characteristic of Fano resonance. The Q factor can, thus, be estimated by fitting the spectrum with the Fano resonance equation described in Eq. (1). The fitted curve is shown in Fig. 4 as the red curve. The extracted Q factor was estimated to be 394, which was close to the calculated value.

Fig. 5(a) shows the polar plot of polarizer angle dependence of PL intensity. The DOP is defined as $(I_{max} - I_{min})/(I_{max} + I_{min})$, where I_{max} and I_{min} are the maximum and the minimum intensities of the lasing peak. The measured DOP was calculated to be 73%. The relative high DOP of HCG SELs can be attributed to the resonance direction of electrical fields only parallel to the grating bar. Fig. 5(b) shows the divergence angle of the laser beam. The output intensity was collected by a fiber with a 600 μm core normal to the sample surface on the rotational stage. The angle resolution of the rotation stage was about 0.5° for divergence angle measurement. The divergence angle was measured to be 12°.

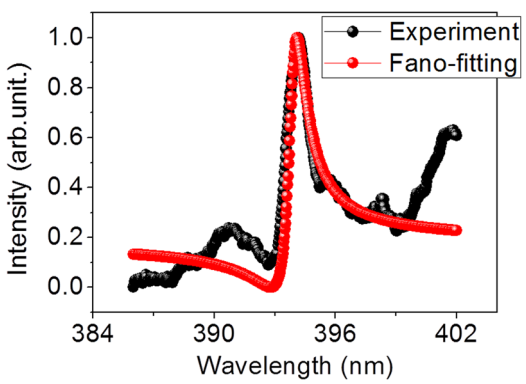

FIG. 4. The PL spectra (black curve) of GaN-based HCG SELs when it was below the threshold condition. The red curve shows the fitting result by Fano-resonance equation. The Q factor was calculated to be 394.

Since the HCG structure can be treated as one dimensional photonic crystal, we can use the PWE method[16] to simulate the photonic band structure of our GaN-based HCG SEL as shown in Fig. 6(a). The normalized frequency of the experimental lasing mode of our GaN-based HCG SEL was located at 0.877, corresponding to the fourth order band in the lower band-edge position in Fig. 6(a). The Bragg scattering of surface emission would occur when the group velocity approached to zero in the fourth order band. The lower band-edge position reveals that the resonance mode in the HCG could be identified as the anti-symmetric mode.[21] In addition, the three dimensional FEM[17] was also used to calculate the mode pattern of GaN-based HCG SEL, as shown in Fig. 6(b). The mode pattern shows several nodes and antinodes which can be referred to the anti-symmetric mode. The simulation also indicates that the AlN/GaN DBRs could provide the mode confinement in the HCG cavity. The resonance direction of electric field is parallel to the grating bar which can match well with the measured DOP results. Furthermore, the anti-symmetric mode would provide good mode confinement in the HCG, resulting in destructive interference in the far-field with little output coupling.[21] The perfect mode confinement supported by Fano resonance could facilitate the high Q factor and the low threshold condition of GaN-based HCG SELs achieved in this experiment.

In summary, GaN-based HCG SELs with AlN/GaN DBRs were demonstrated at room temperature. The low threshold energy density supported by the Fano resonance was measured to be 0.56 mJ/cm^2 and the lasing wavelength was 393.6 nm. The Fano resonance spectra were confirmed and the quality factor was extracted to be 394. Moreover, the lasing characteristics such as the divergence angle and degree of polarization were measured to be 12° and 73%, respectively. Finally, the specific surface emitting lasing mode matched well with the one dimensional photonic band diagram and mode pattern. Since GaN-based SELs have drawn much attention due to many practical applications including laser display, laser printer, high density optical storage, and the next generation micro/pico-projectors, we

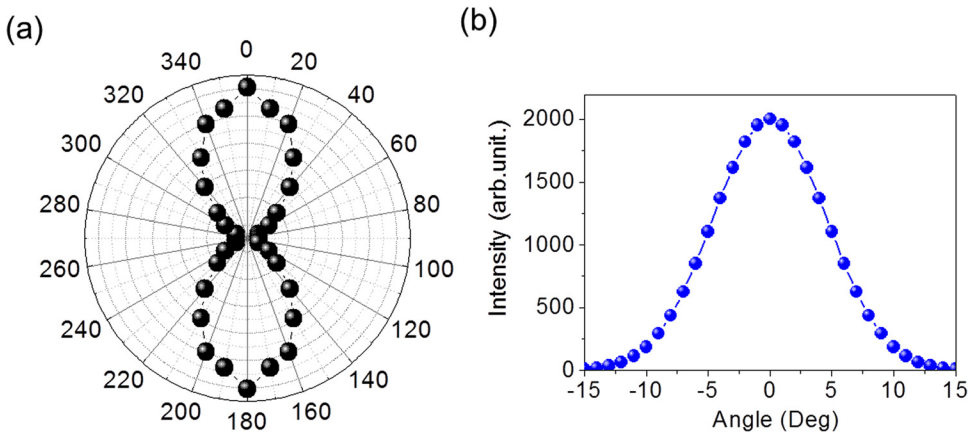

FIG. 5. (a) The DOP and (b) the divergence angle of the GaN-based HCG SEL when it was above the threshold condition. The detection direction was normal to the surface of the GaN-based HCG SEL. The DOP and divergence angle were measured to be 73% and 12°, respectively.

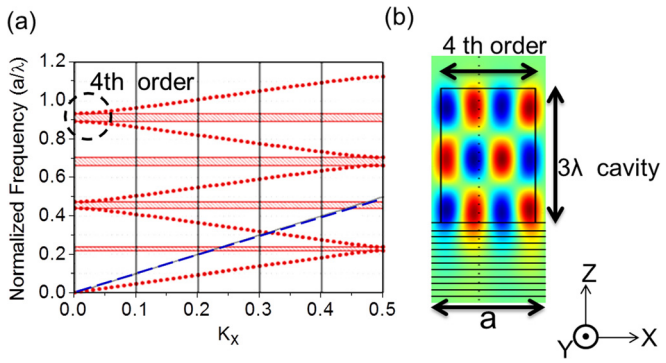

FIG. 6. (a) The calculated band structure of GaN-based HCG SEL using the PWE method. The blue dashed line represents the light line. The red dotted lines represent the different order bands and the black circle indicates the forth order band. (b) The calculated pattern of 4th order mode in the GaN-based HCG SEL using the finite element method. The parameter *a* is the grating period.

believe GaN-based HCG SELs can be the best candidate for accomplishment of low threshold, high power short wavelength coherent light sources in the near future.

The authors would like to gratefully acknowledge Professor Koyama at Tokyo Institute of Technology for his fruitful suggestion and Professor H. C. Kuo at National Chiao Tung University for his technical support. This work was supported in part by the Ministry of Education Aim for the Top University program and by the National Science Council of Taiwan under Contract Nos. NSC99-2622-E009-009-CC3 and NSC98-2923-E-009-001-MY3.

[1]C. F. R. Mateus, M. C. Y. Huang, Y. Deng, A. R. Neureuther, and C. J. Chang-Hasnain, IEEE Photon. Technol. Lett. **16**, 518 (2004).
[2]M. C. Y. Huang, Y. Zhou, and C. J. Chang-Hasnain, Nat. Photonics **1**, 119 (2007).
[3]M. C. Y. Huang, Y. Zhou, and C. J. Chang-Hasnain, Nat. Photonics **2**, 180 (2008).
[4]V. Karagodsky, B. Pesala, C. Chase, W. Hofmann, F. Koyama, and C. J. Chang-Hasnain, Opt. Express **18**, 694 (2010).
[5]C. Chase, Y. Rao, W. Hofmann, and C. J. Chang-Hasnain, Opt. Express **18**, 15461 (2010).
[6]Y. Zhou, M. C. Y. Huang, C. Chase, V. Karagodsky, M. Moewe, B. Pesala, F. G. Sedgwick, and C. J. Chang-Hasnain, IEEE J. Sel. Top. Quantum Electron. **15**, 1485 (2009).
[7]Y. Zhou, M. Moewe, J. Kern, M. C. Y. Huang, and C. J. Chang-Hasnain, Opt. Express **16**, 17282 (2008).
[8]T. C. Lu, S. W. Chen, T. T. Wu, P. M. Tu, C. K. Chen, C. H. Chen, Z. Y. Li, H. C. Kuo, and S. C. Wang, Appl. Phys. Lett. **97**, 071114 (2010).
[9]T. C. Lu, T. T. Wu, S. W. Chen, P. M. Tu, Z. Y. Li, C. K. Chen, C. H. Chen, H. C. Kuo, S. C. Wang, H. W. Zan, and C. Y. Chang, IEEE J. Sel. Top. Quantum Electron. **17**, 1594 (2011).
[10]D. Kasahara, D. Morita, T. Kosugi, K. Nakagawa, J. Kawamata, Y. Higuchi, H. Matsumura, and T. Mukai, Appl. Phys. Express **4**, 072103 (2011).
[11]H. Matsubara, S. Yoshimoto, H. Saito, Y. Jianglin, Y. Tanaka, and S. Noda, Science **319**, 445 (2008).
[12]T. C. Lu, S. W. Chen, L. F. Lin, T. T. Kao, C. C. Kao, P. Yu, H. C. Kuo, S. C. Wang, and S. H. Fan, Appl. Phys. Lett. **92**, 011129 (2008).
[13]T. T. Wu, P. S. Weng, Y. J. Hou, and T. C. Lu, Appl. Phys Lett. **99**, 221105 (2011).
[14]S. Kawashima, T. Kawashima, Y. Nagatomo, Y. Hori, H. Iwase, T. Uchida, K. Hoshino, A. Numata, and M. Uchida, Appl. Phys. Lett. **97**, 251112 (2010).
[15]J. Kim, D. U. Kim, J. H. Lee, H. S. Jeon, Y. S. Park, and Y. S. Choi, Appl. Phys. Lett. **95**, 021102 (2009).
[16]S. H. Kwon, H. Y. Ryu, G.-H. Kim, Y. H. Lee, and S. B. Kim, Appl. Phys. Lett. **83**, 3870 (2003).
[17]J. Jin, *The Finite Element Method in Electromagnetics* (Wiley, New York, 2002).
[18]M. G. Moharam and T. K. Gaylord, J. Opt. Soc. Am. **71**, 811 (1981).
[19]U. Fano, Phys. Rev. **124**, 1866 (1961).
[20]M. V. Rybin, M. V. Rybin, A. B. Khanikaev, M. Inoue, A. K. Samusev, M. J. Steel, G. Yushin, and M. F. Limonov, Photonics Nanostruct. Fundam. Appl. **8**, 86 (2010).
[21]S. L. Chua, Y. D. Chong, A. Douglas Stone, M. Soljačić, and J. Bravo-Abad, Opt. Express **19**, 1539 (2011).